

GSA Data Repository Item **2015003** accompanies

Schoenbohm, L.M., and Carrapa, B., 2015, Miocene–Pliocene shortening, extension, and mafic magmatism support small-scale lithospheric foundering in the central Andes, NW Argentina, *in* DeCelles, P.G., Ducea, M.N., Carrapa, B., and Kapp, P.A., eds., *Geodynamics of a Cordilleran Orogenic System: The Central Andes of Argentina and Northern Chile*: Geological Society of America Memoir 212, p. 167–180, doi:10.1130/2015.1212(09).

Supplementary Data

U-Pb Geochronology by LA-MC-ICPMS at the Arizona LaserChron Center

U-Pb geochronology for the three Arizaro samples (Table 1 and Fig. 1) was conducted using laser ablation multi-collector inductively coupled plasma mass spectrometry (LA-MC-ICPMS) at the LaserChron Center at the University of Arizona, following the methods of Gehrels et al. (2008). Zircons were separated from the collected samples using standard methods, glued to mounts, polished and imaged using cathode luminescence to ensure that only zircon grains were chosen for analysis. Analyses involve ablation with a New Wave DUV193 Excimer laser using generally a spot diameter of 35 microns and ~15 micron depth. Each analysis consists of one 20-second integration on peaks with the laser off (for backgrounds), 12 one-second integrations with the laser firing, and a 30 second delay to purge the previous sample and prepare for the next analysis. Ablated material is carried via helium gas into a GVI Isoprobe, where isotopes of U, Th and Pb are measured simultaneously by Faraday detectors with 10e11 ohm resistors for ^{238}U , ^{232}Th , ^{208}Pb , and ^{206}Pb , a Faraday detector with a 10e12 ohm resistor for ^{207}Pb , and an ion-counting channel for ^{204}Pb . Ion yields are ~1 mv per ppm. Errors in determining $^{206}\text{Pb}/^{238}\text{U}$ and $^{206}\text{Pb}/^{207}\text{Pb}$ result in $^{206}\text{Pb}/^{238}\text{U}$ age errors between 1% and 10%. Errors for $^{206}\text{Pb}/^{207}\text{Pb}$ ages are generally lower than error for $^{206}\text{Pb}/^{238}\text{U}$ ages of the same grains. Ages reported are $^{206}\text{Pb}/^{238}\text{U}$ ages. An initial Pb composition from Stacey and Kramers (1975) is assumed in order to account for common Pb with uncertainties of 1.0 for $^{206}\text{Pb}/^{204}\text{Pb}$, 0.3 for $^{207}\text{Pb}/^{204}\text{Pb}$, and 2.0 for $^{208}\text{Pb}/^{204}\text{Pb}$. Background ^{204}Pb and ^{204}Hg are accounted for by subtracting background intensity from peak intensity. U-Pb ages for <10 Ma grains have been corrected for U-Th disequilibrium following Crowley et al. (2007). Th/U for the zircon crystals is from the measured values, whereas Th/U for the magma is assumed to have a typical igneous value of 2. Secular equilibrium is also assumed. Decay constants are 15.5e-11 for ^{238}U and 9.2e-6 for ^{230}Th . This correction results in ages that are an average of 0.04 Ma older than the uncorrected ages, which is negligible considering the large uncertainty of each age determination. The ages reported in Table 2 [at end of this file] are accordingly not corrected for U-Th disequilibrium. The fractionation standard used in all analyses was a large zircon crystal from Sri Lanka, which yields an age of 565.3 ± 3.2 Ma from ID-TIMS by Gehrels et al. (2008). Concentrations of U, Th, and Pb from unknown sample grains are determined to within ~20% accuracy by comparing intensities to those from the Sri Lankan standard, which has known U, Th, and Pb concentrations. Data are filtered for precision (10% cutoff) and concordance (30% cutoff). Full analytical data can be found in Table DR2 and Figure DR3. Uncertainties are reported to 1 σ levels, and represent analytical errors. Calculations of weighted mean, weighted mean error, and MSWD are in Figure 3 and in the text are from Bevington and Robinson (2002) and McDougall and Harrison (1988). For more information concerning lab methods at the Arizona LaserChron center, refer to Gehrels et al. (2008).

U-Pb Geochronology by Ion Microprobe at the UCLA SIMS Center

U-Pb geochronology (Table 2) for the three Pasto Ventura samples (PVN75, PVN226 and PVN260) was conducted using the Cameca IMS1270 ion microprobe at the University of California, Los Angeles SIMS Center. Zircons were separated from the collected ashes using standard methods. Grain mounts of hand-selected zircons were coated with gold and were probed with a mass-filtered 10-20 nA 160 beam focused to a 30-35 μm diameter spot size. U-Pb ratios were determined relative to a calibration curve based on reference zircon AS-3 (Paces and Miller, 1993). We analyzed between 13 and 18 grains per sample (Table 2). After making exclusions, ZIPS 3.0 (in-house software developed by Chris Coath) was used to reduce data using an isochron regression. More details on this method can be found in Schmitt et al. (2003). Sample PVN-75 contains a uniform population of zircons with an age of 10.5 ± 0.1 Ma (MSWD = 0.63). Sample PVN-226 and PVN-260 both had large populations clustered around ~ 10 Ma, but both contained at least one zircon with a younger age. The ages are geologically reasonable and therefore cannot be excluded on the basis of contamination. The older population likely reflects reworking from a large eruption, but we consider the younger ages to be the true sample ages. PVN-226 yields an age of 7.88 ± 0.58 Ma on the basis of a single grain and PVN-260 yields an age of 7.77 ± 0.21 (MSWD = 0.05) on the basis of two grains.

$^{40}\text{Ar}/^{39}\text{Ar}$ Geochronology

$^{40}\text{Ar}/^{39}\text{Ar}$ analyses (Figs. 2-10) were performed at the USGS in Denver, Colorado. Samples were prepared by crushing and isolating chips approximately 1 mm^3 from fresh rock free of obvious alteration and phenocrysts. The basalt chips were washed in deionized water and together with standards, were irradiated for 20 megawatt hours in the central thimble position of the USGS TRIGA reactor using cadmium lining to prevent nucleogenic production of ^{40}Ar . The neutron flux was monitored using Fish Canyon Tuff sanidine, using an age of $28.20 \text{ Ma} \pm 0.08 \text{ Ma}$ (Kuiper et al. 2008) and isotopic production ratios were determined from irradiated CaF_2 and KCl salts. For this irradiation, the following production values were measured: $(^{36}/^{37}\text{Ca}) = 2.447 \times 10^{-4} \pm .47$; $(^{39}/^{37}\text{Ca}) = 6.5 \times 10^{-4} \pm 0.53$; and $(^{38}/^{39}\text{K}) = 1.29 \times 10^{-2} \pm 0.01$. The irradiated basalt samples and standards were loaded into 3 mm wells within a stainless steel planchette attached to a fully automated ultra-high vacuum extraction line constructed of stainless steel. Samples were incrementally degassed using a 20W CO_2 laser equipped with a beam homogenizing lens. The gas was expanded and purified by exposure to a cold finger maintained at -140°C and two hot SAES GP50 getters. Following purification the gas was expanded into a Mass Analyser Products 215-50 mass spectrometer and argon isotopes were measured by peak jumping using an electron multiplier operated in analog mode. Data were acquired during 10 cycles and time zero intercepts were determined by best-fit regressions to the data. Data were corrected for mass discrimination, blanks, radioactive decay subsequent to irradiation, and interfering nucleogenic reactions.

References

- Bevington, P.R. and Robinson, D.K. *Data reduction and error analysis for the physical sciences*. McGraw Hill, New York, 336 pp. (2002).
- Crowley, J., Schoene, B., and Bowring, S. U-Pb dating of zircon in the Bishop Tuff at the millennial scale. *Geology* **35** 1123-1126 (2007).
- Gehrels, G. E., V. A. Valencia, and J. Ruiz. Enhanced precision, accuracy, efficiency, and spatial resolution of U-Pb ages by laser ablation–multicollector–inductively coupled plasma–mass spectrometry. *Geochem. Geophys. Geosyst.* **9** Q03017 (2008).
- Kuiper, K.F., Deino, A., Hilgen, F.J., Krijgsman, W., Renne, P.R., and Wijbrans, J.R. Synchronizing Rock Clocks of Earth History. *Science* **320** 500-504 (2008).
- McDougall, I. and Harrison, T.M. Geochronology and thermochronology by the $^{40}\text{Ar}/^{39}\text{Ar}$ method. In: *Oxford Monographs on Geology and Geophysics*. Oxford University Press, Oxford. **9** 212 (1988).
- Paces, J.B., and Miller, J.D. Precise U-Pb ages of Duluth Complex and related mafic intrusions, northeastern Minnesota: geochronological insights to physical, petrogenetic, paleomagnetic, and tectonomagnetic processes associated with the 1.1 Ga Midcontinent Rift System. *J. Geophys. Rsrch.* **98** 13,997-14013 (1993).
- Schmitt, A.K., Grove, M., Harrison, T.M., Lovera, O., Hulen, J., and Walters, M. The Geysers-Cobb Mountain magma system, California (Part 1): U-Pb zircon ages of volcanic rocks, conditions of zircon crystallization and magma residence times. *Geochim. et Cosmochim. Acta.* **67** 3423-3442 (2003).
- Stacey, J.S. and Kramers, J.D. Approximation of Terrestrial Lead Isotope Evolution by a 2-Stage Model. *Earth and Planet. Sci. Letters.* **26** 207-221 (1975).

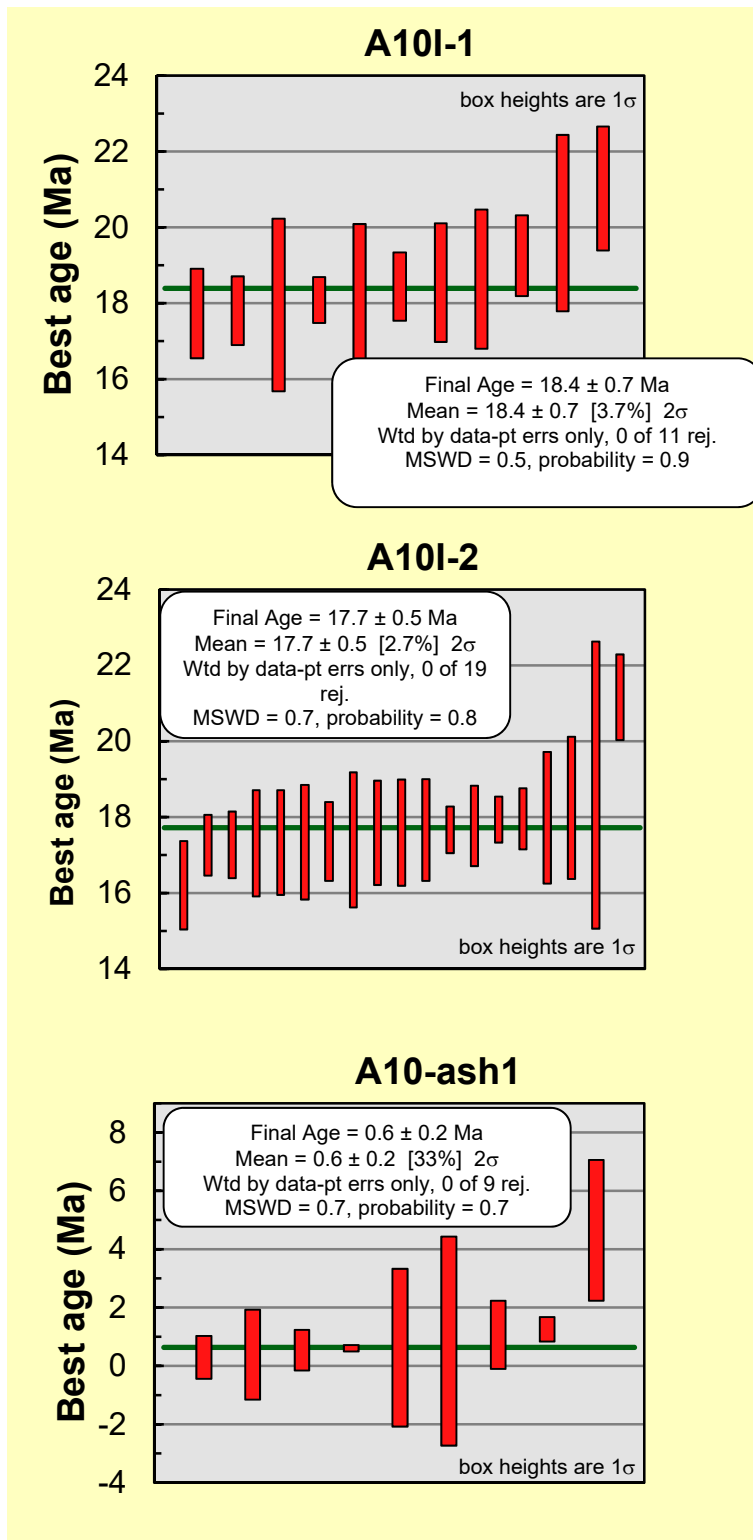


Figure 1. Plots of best ages for ignimbrite (A10I-1 and A10I-2) and ash (A10-ash1) samples from the western margin of the Salar de Arizaro. See Table 2 for additional details.

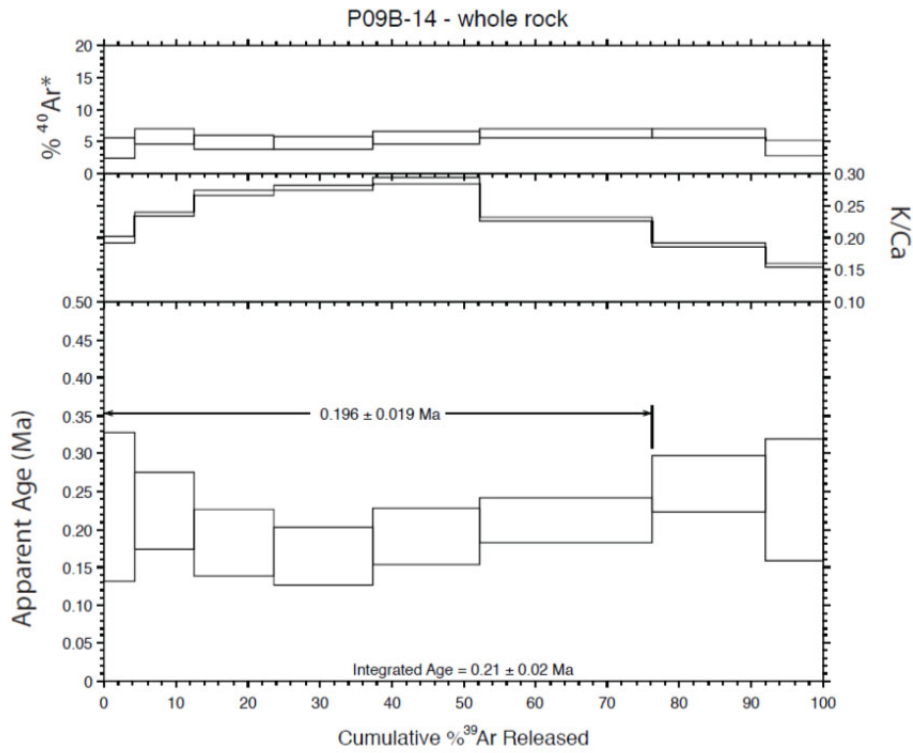


Figure 2. $^{40}\text{Ar}/^{39}\text{Ar}$ step heating data for sample A09B-14. Location: S24.56277, W67.90611.

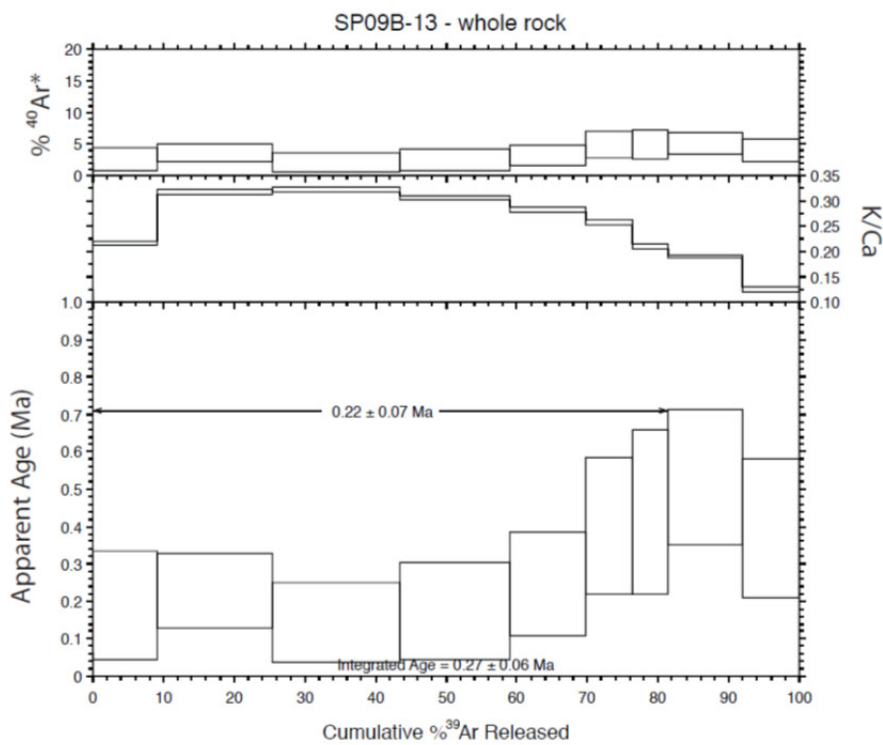


Figure 3. $^{40}\text{Ar}/^{39}\text{Ar}$ step heating data for sample A09B-13. Location: S24.70549, W67.93403.

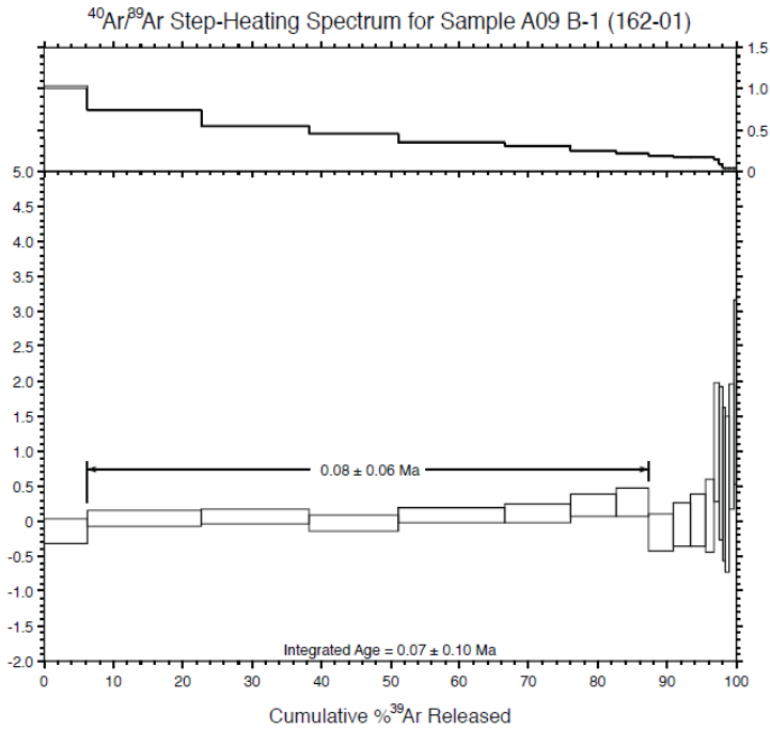


Figure 4. ⁴⁰Ar/³⁹Ar step heating data for sample A09B-1. Location: S24.7002, W 67.9826.

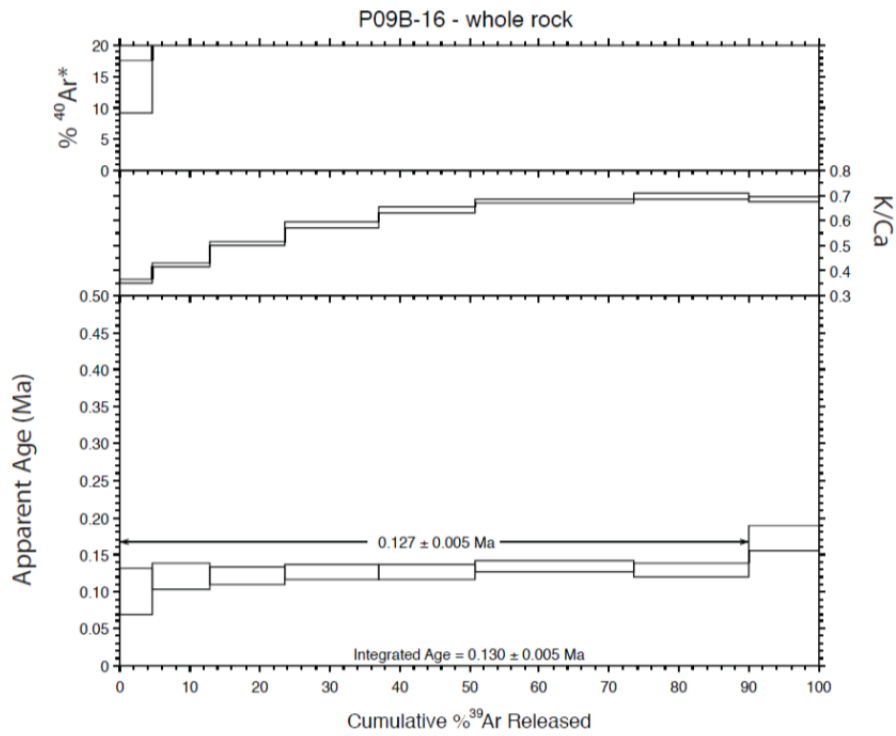


Figure 5. ⁴⁰Ar/³⁹Ar step heating data for sample A09B-16. Location: S24.81355, W68.05165.

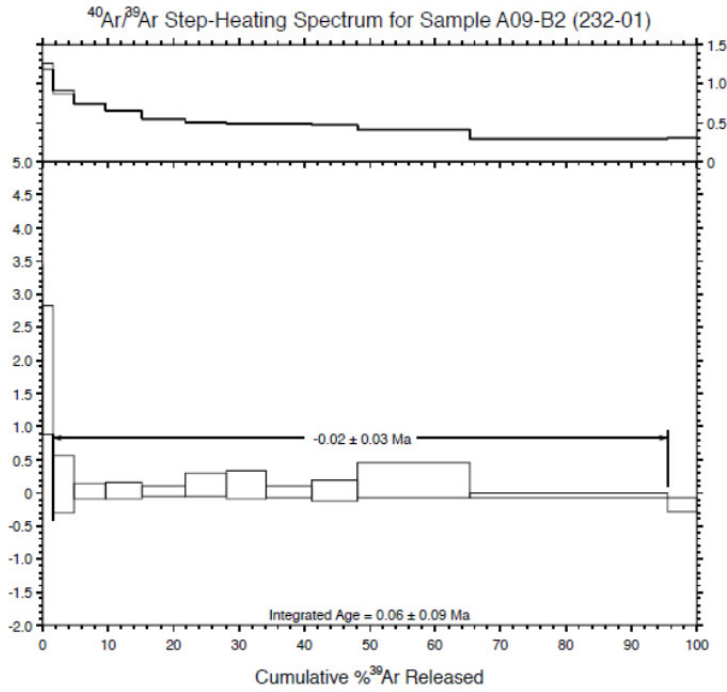


Figure 6. ⁴⁰Ar/³⁹Ar step heating data for sample A09B-2. Location: S25.1429, W67.6099.

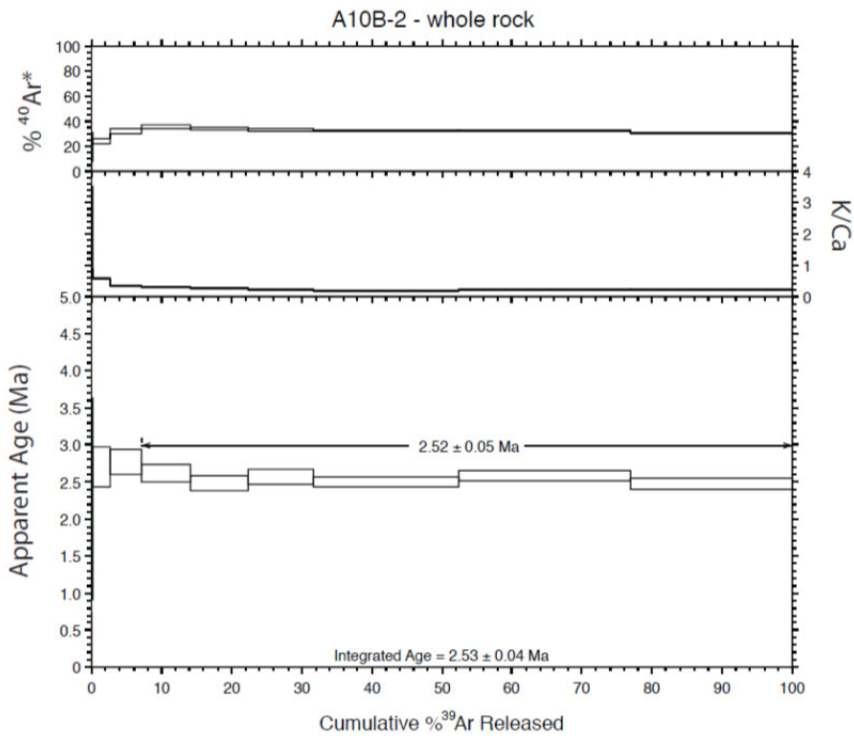


Figure 7. ⁴⁰Ar/³⁹Ar step heating data for sample A10B-2. Location: S24.75990, W68.03572.

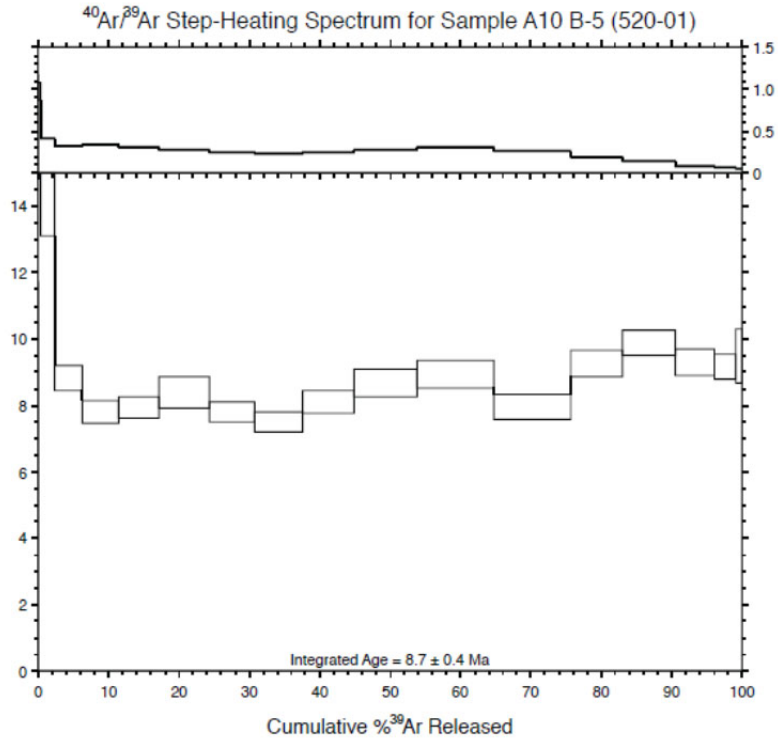


Figure 8. $^{40}\text{Ar}/^{39}\text{Ar}$ step heating data for sample A10B-5. Location: S25.9239, W67.7090.

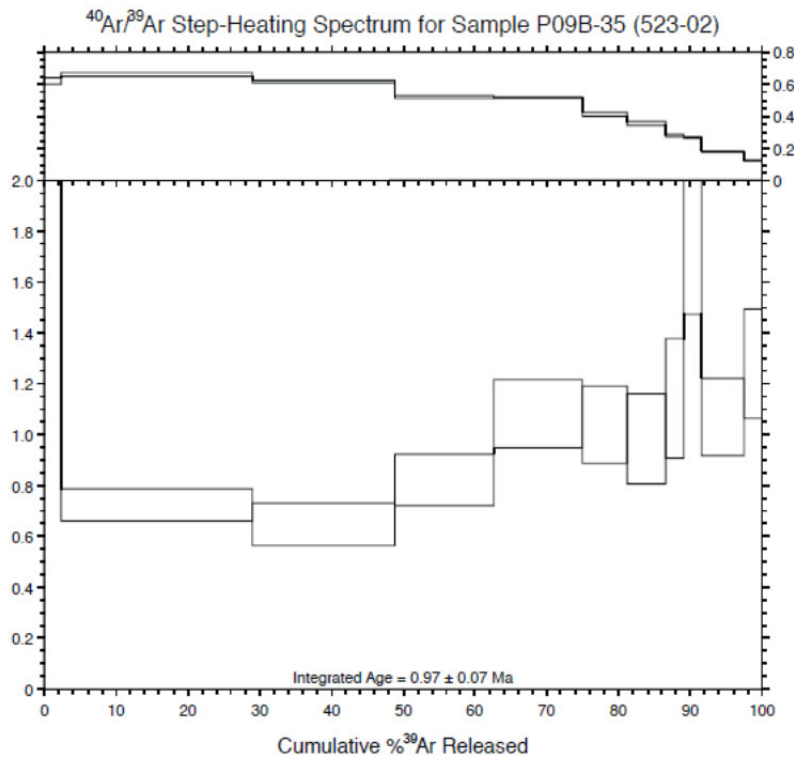
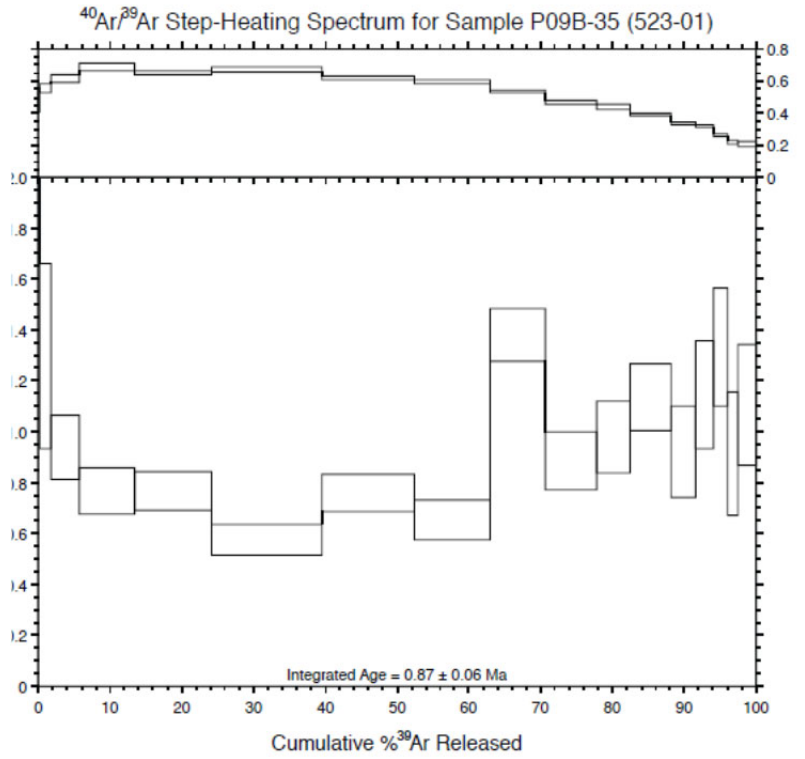


Figure 9. ⁴⁰Ar/³⁹Ar step heating data for two replicates of sample A09B-35. Location: S25.2643, W67.0684.

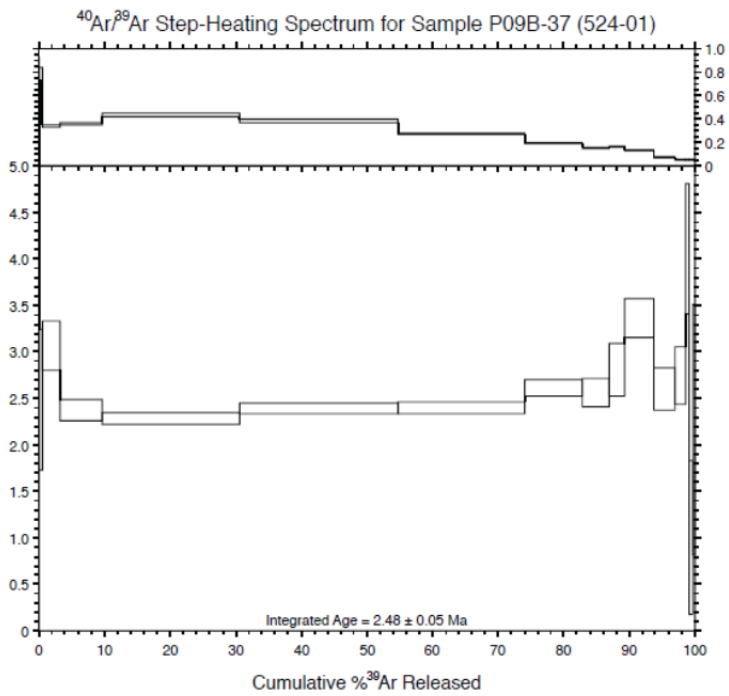
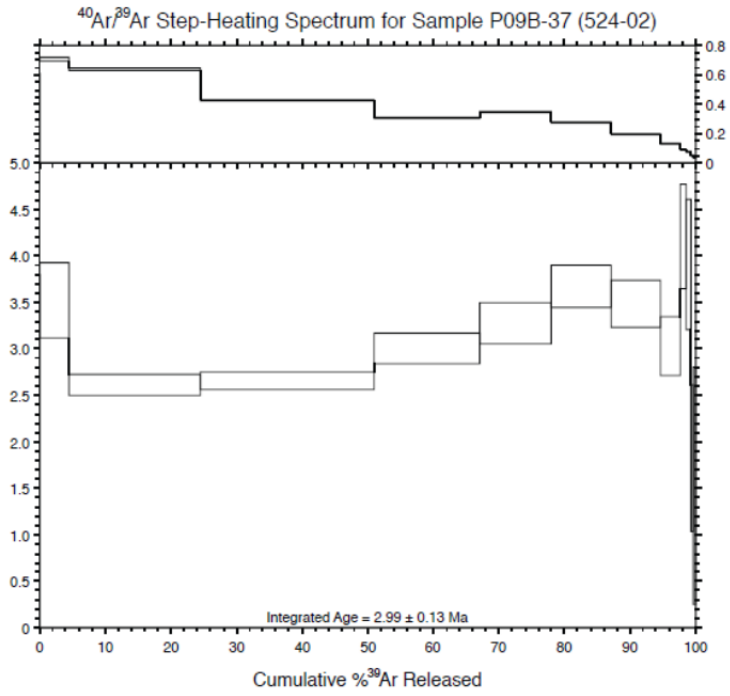


Figure 10. ⁴⁰Ar/³⁹Ar step heating data for two replicates of sample A09B-37. Location: S25.1978, W67.0072

Table 2. U-Pb dating of Pasto Ventura ashes using the UCLA SIMS facility

Sample name	U (ppm)	238U/206Pb		207Pb*/206Pb*		Correl. of Ellipses	UO/U	% 206Pb*	206/238	
		value	1 s.e.	value	1 s.e.				Age (Ma)	1 s.e.
PVN75sp1	570	602.4	23.0	0.0746	0.0034	-0.09	9.0	96.4	10.4	0.41
PVN75sp2	1692	610.1	23.8	0.0490	0.0020	-0.03	8.9	99.6	10.6	0.41
PVN75sp3	1171	621.9	26.0	0.0526	0.0023	0.02	8.8	99.2	10.4	0.43
PVN75sp4	348	592.1	25.2	0.0688	0.0061	-0.01	8.9	97.1	10.6	0.47
PVN75sp5	1251	633.3	25.5	0.0594	0.0025	0.01	8.9	98.3	10.1	0.41
PVN75sp6	1602	600.6	26.1	0.0538	0.0021	-0.07	8.8	99.0	10.7	0.47
PVN75sp7	233	625.8	33.0	0.0774	0.0128	0.10	8.7	96.0	9.97	0.56
PVN75sp8	1767	601.0	26.0	0.0487	0.0018	-0.03	8.7	99.7	10.8	0.46
PVN75sp9	819	627.7	29.4	0.0524	0.0031	0.01	8.6	99.2	10.3	0.48
PVN75sp10	3130	567.5	24.6	0.0499	0.0016	0.18	9.0	99.5	11.4	0.49
PVN75sp11	783	606.8	26.1	0.0539	0.0038	-0.12	8.9	99.0	10.6	0.46
PVN75sp12	498	618.0	26.6	0.0542	0.0051	0.08	8.8	99.0	10.4	0.45
PVN75sp13	415	635.7	27.4	0.0657	0.0045	-0.02	8.8	97.5	9.97	0.44
								w.m.	10.5	
								±1σ	0.1	
								MSWD	0.63	
PVN226sp1	51	548.5	37.0	0.1990	0.0284	-0.21	8.8	80.5	9.54	0.93
PVN226sp2	96	615.0	39.0	0.1149	0.0151	0.15	8.6	91.2	9.63	0.69
PVN226sp3	2509	636.1	25.7	0.0527	0.0018	0.02	8.8	99.2	10.1	0.4
PVN226sp4	110	690.1	36.7	0.1744	0.0245	0.00	8.9	83.6	7.88	0.58
PVN226sp5	764	549.5	24.4	0.0573	0.0031	-0.08	8.7	98.6	11.7	0.5
PVN226sp6	151	567.5	33.8	0.1204	0.0131	-0.19	8.7	90.5	10.4	0.7
PVN226sp7	49	519.8	33.2	0.1884	0.0205	-0.24	8.8	81.8	10.2	0.9
PVN226sp8	79	552.8	32.1	0.1528	0.0164	0.06	8.7	86.4	10.1	0.7
PVN226sp9	56	432.9	26.8	0.2706	0.0261	-0.05	8.8	71.3	10.7	1.1
PVN226sp10	70	544.7	35.6	0.1347	0.0146	-0.20	8.8	88.7	10.6	0.8
PVN226sp11	385	641.4	27.3	0.0785	0.0053	-0.06	8.8	95.9	9.73	0.43
PVN226sp12	224	621.5	29.7	0.0840	0.0123	-0.17	8.7	95.2	9.95	0.52
PVN226sp13	429	656.6	31.3	0.0755	0.0094	0.07	8.6	96.3	9.52	0.48
PVN226sp14	83	567.9	31.6	0.1254	0.0137	0.05	8.9	89.9	10.3	0.7
PVN226sp15	299	570.1	27.5	0.0752	0.0116	0.06	8.5	96.3	11.0	0.6
								w.m.	7.88	
								±1σ	0.58	
								MSWD	n/a	
PVN260sp1	684	460.4	18.4	0.3357	0.0112	-0.06	9.2	63.0	8.91	0.64
PVN260sp3	772	660.1	21.0	0.2181	0.0138	0.13	10.5	78.0	7.71	0.35
PVN260sp4	1137	441.9	14.8	0.1773	0.0078	0.13	10.4	83.2	12.19	0.51
PVN260sp5	2895	668.4	17.2	0.2016	0.0063	0.06	10.4	80.1	7.81	0.26
PVN260sp6	865	447.2	12.9	0.1466	0.0063	-0.02	10.3	87.2	12.63	0.44
PVN260sp7	1714	515.5	15.6	0.1286	0.0053	0.12	10.4	89.5	11.25	0.39
PVN260sp8	2155	497.0	12.7	0.1156	0.0046	-0.08	10.6	91.1	11.91	0.38
PVN260sp9	821	424.4	12.0	0.1648	0.0078	0.08	10.4	84.8	12.95	0.46
PVN260sp10	747	525.2	19.5	0.2123	0.0088	0.00	10.4	78.8	9.75	0.49
PVN260sp11	762	569.2	22.4	0.1584	0.0058	0.05	9.2	85.6	9.78	0.46
PVN260sp13	180	361.8	15.7	0.0736	0.0069	0.12	9.1	96.5	17.24	0.79
PVN260sp14	542	656.6	27.4	0.0699	0.0071	0.10	9.1	97.0	9.60	0.42
PVN260sp15	364	377.6	13.8	0.0620	0.0063	-0.20	9.3	98.0	16.78	0.64
PVN260sp16	937	658.3	27.7	0.0573	0.0027	0.03	8.8	98.6	9.74	0.41
PVN260sp17	807	646.4	26.7	0.0525	0.0028	-0.08	8.8	99.2	9.98	0.41
PVN260sp19	975	610.9	25.9	0.0875	0.0052	-0.05	8.7	94.7	10.08	0.46

PVN260sp20	75	578.7	33.1	0.0952	0.0147	-0.19	8.7	93.7	<i>10.51</i>	<i>0.67</i>
PVN260sp21	774	640.2	25.7	0.0606	0.0030	-0.06	8.8	98.2	<i>9.96</i>	<i>0.41</i>
								w.m.	7.77	
								±1σ	0.21	
								MSWD	0.05	

^aGrey, italicized ages were excluded from the weighted mean age for each ash.